ESSB-2017-05

MEBT-BI-BC91-04

General Technical Report of Beam Current Monitors (BCM) of MEBT

S. Varnasseri, I. Bustinduy, J. Martin, A. Conde, A. Zugazaga, I. Rueda

6 May, 2017

Project: MEBT
Version: 4.0
Approved by: I. Bustinduy
Revised by: I. Rueda

Change History

Rev.	Date	Author(s)	Description
0.0	2017-05-08	S. Varnasseri	First Version
0.1	2017-05-10		Edition in vacuum section
0.2	2017-05-25		Organizational and other editions
0.3	2017-05-31		Verifications minor change 8.2
0.4	2017-06-21		Minor changes in Section.7 and Section. 9

Table of Contents

1. INTRODUCTION

For the purpose of beam current measurement in terms of fast and slow time resolution, two ACCTs and one FCT are placed in two locations of the MEBT. There is an additional ACCT at the entrance of the MEBT, this ACCT is part of the RFQ, and is out of the scope of the present report.

Figure.1 shows the location of ACCT1, ACCT2 and FCT in the MEBT layout.

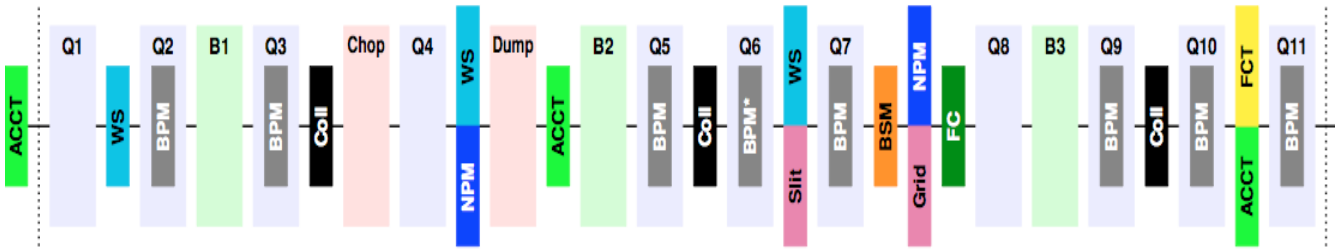

Figure. 1: Location of ACCTs and FCT in the MEBT instrumentation.

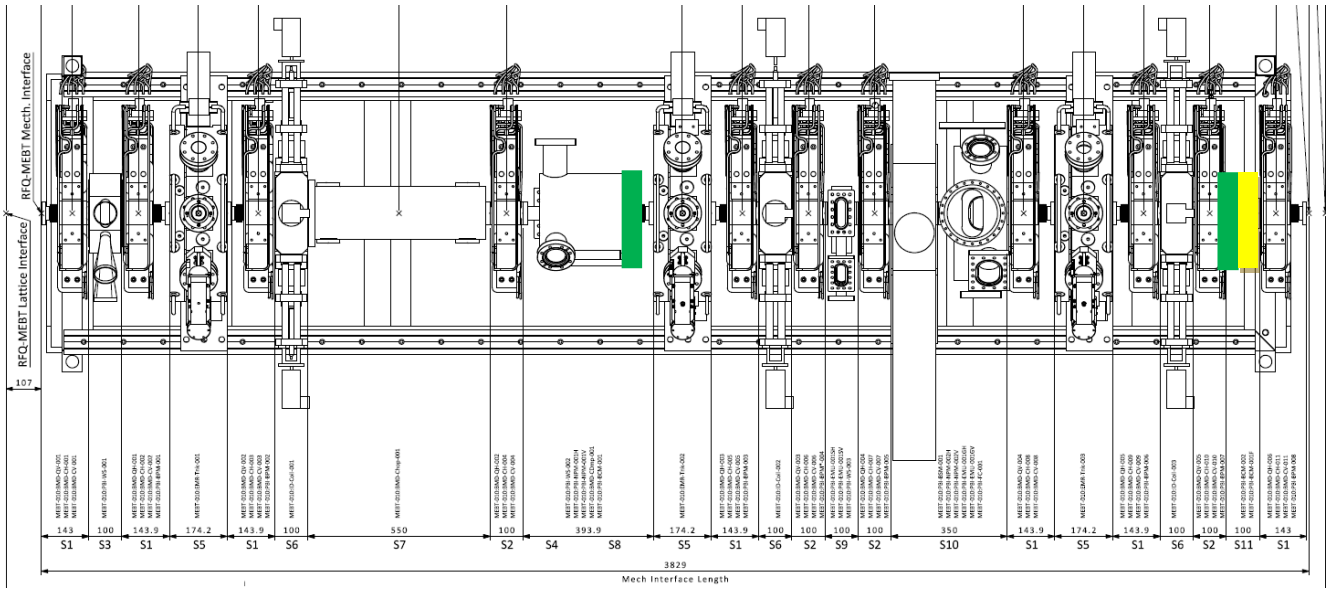

Figure. 2: Layout of MEBT and reserved locations of ACCTs (green), FCT(yellow).

2. GENERAL REQUIREMENTS

Table. 1 shows the general requirements of the ACCTs. It shows the parameters to be measured and their expected values, limits or resolutions. Since fulfilment of some parameters requires access to the whole system from sensor to the acquisition and processing, then parts of the verifications are carried out by Bilbao, mainly the ones related to the mechanical parts and the specific ones related to cabling and control integration are carried out by ESS Lund (see Table. 1 for more details).

Table.1 : General requirements for BCMs

Ref.	Parameter	Values / Description	**Bilbao**	**ESS**
MEBT-L4-PBI-010	Operating domain: beam current range	All measurements in the MEBT shall be done over a beam current range from 1 mA to the nominal	Toroid, Analogue Electronics	Acquisition, ICS
MEBT-L4-PBI-030	Operating domain for non-interceptive measurements: beam repetition frequency range	All non-interceptive measurements in the MEBT shall be possible for all the repetition frequency modes ranging from pulse on demand to 14 Hz	Toroid, Analogue Electronics	Acquisition, ICS
MEBT-L4-PBI-070	Beam current measurement: accuracy	Beam currents shall be measured with an accuracy better than ± 1 mA	Toroid, Analogue Electronics	Acquisition, ICS
MEBT-L4-PBI-080	Beam current measurement: resolution	Beam currents shall be measured with a resolution better than 1% of the peak beam current	-	Acquisition,
MEBT-L4-PBI-100	Beam current measurement: time resolution	Beam currents shall be measured with a time resolution better than 1 micro-second.	Toroid, Analogue Electronics	Acquisition, ICS
MEBT-L4-PBI-220	Beam loss measurement: MPS detection threshold	A beam current loss of 10 % of the nominal peak beam current over a period of 10 μs shall be detected in the MEBT	Toroid, Analogue Electronics	Acquisition, ICS

3. **MEBT BCM'S SPECIFIC REQUIREMENTS**

Table.2 shows the main measurement specifications of the ACCT1/ACCT2/FCT toroids. ACCTs will be used for the beam pulse current measurements of the MEBT. From the data collected of ACCTs, one can find the average beam loss and transmission efficiency of the MEBT. FCT will be used for fast timing characteristics of beam such as monitoring the rise/fall time of the beam Chopper.

Table. 2: Main measurement specifications of toroids

ACCT bandwidth (3 dB)	≥1 MHz
ACCT lower cut-off (3 dB)	3 Hz
Beam current (nominal)	80 mA
Electronics full scale range	±10 V
FCT bandwidth	>352 MHz
FCT readout rise/fall time	<10 ns

4. VARIOUS OPTIONS FOR BCM'S

The general method of multi layer shielding has been utilized in the current transformer shielding design. For the outer layer, low-permeability and high-field saturation steel is used, while for the inner shielding high-permeability and low-field saturation Mu-metal is used.

4.1. ACCT1

For the ACCT1, the mechanical and integration factors dictate the outer dimension of the toroid. A study has been performed in order to evaluate the necessity of the magnetic and radiation shielding for the toroid [3,4]. The study shows the value of absolute external magnetic field is less than 0.5 Gauss. This is due to long distance from quadrupoles Q4, Q5.

In-Air model of toroid is chosen. The electrical gap has been introduced with EPDM gasket. In this solution, the bypass current is rooted via the outer part of the flange to body of beam dump (see fig. 3).

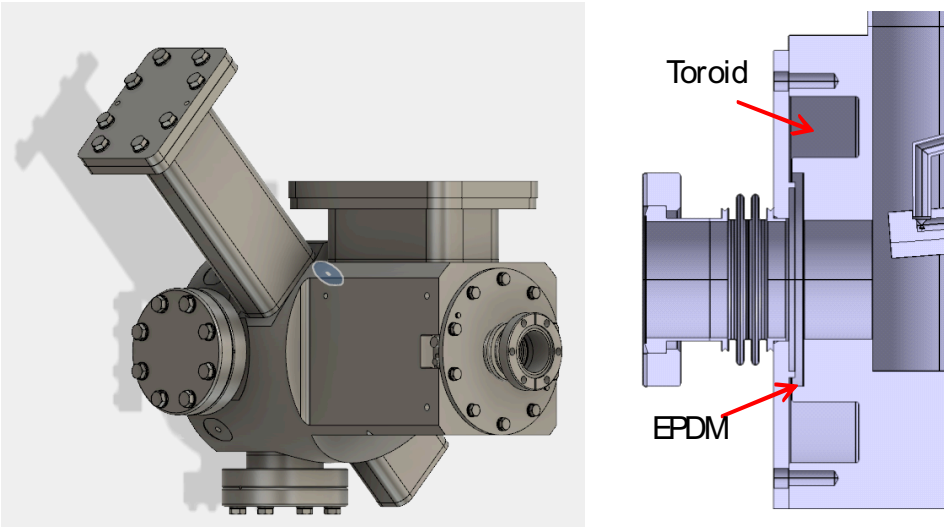

Figure 3: Location of ACCT1 downstream of the beam dump vessel, and a close up view of the toroid with the corresponding EPDM gasket seal.

4.1.1. EXTERNAL MAGNETIC FIELD

Qaudrupole magnets (Q4, Q5) as the external magnetic field sources have been considered in order to evaluate the intensity of magnetic field in the location of ACCT1 toroid.

Table.3: External magnetic field sources for ACCT1

Quadrupoles field data		
Q4 Gradient	5 T/m	+20%
Q5 Gradient	6.5 T/m	+20%
ACCT1 distance from Q4	373 mm	
ACCT1 distance from Q5	339 mm	

Fig. 4 shows the superimposed external magnetic field due to adjacent quadrupoles (i.e Q4, Q5) in the location of ACCT1 toroid. The plot surface is perpendicular to the beam direction and x,y correspond to transverse coordinates.

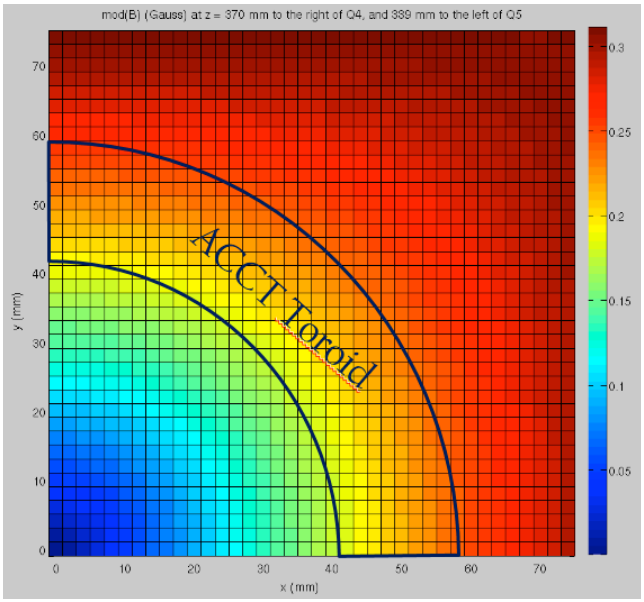

Figure.4: External magnetic field map at the location of ACCT1 toroid without shielding.

The values of external magnetic field are less than 0.5 Gauss. This value is much lower than the external magnetic field limit for the toroids saturation. Therefore, no magnetic shielding is foreseen for the ACCT1.

4.1.2. RADIATION ASPECTS

The study of the radiation levels for various devices of MEBT has been performed [4]. The calculation shows the radiation level in the location of ACCT1 toroid is safely less than the radiation resistance of the vulnerable ACCT standard sensor materials like silicon rubber SIR or wiring insulation of $2x10^5$ Gy. As a result of the study, no radiation shielding except the already beam dump and flange stainless steel

structure around the ACCT1 has been considered. For the radiation safety purposes, the calibration connector insulation is PEEK material instead of PTFE.

4.2. COMBINED ACCT2 AND FCT (COMBO)

Due to short longitudinal space and integration limitations, it is decided to combine the ACCT2 and FCT in a vertical reference line (i.e Combo design). In principle, there is no problem of inter talks between the two toroids, since they are working in separate frequency bands. However, constructing the magnetic shield and insulation gap on the tube could produce some unwanted noises or resonances on the signal of FCT. Two options of In-Air and In-flange solutions have been studied. The integrated external magnetic field data has been given in section 4.2.1. Table. 4 shows the external field sources considered with margin for the magnetic field shielding analysis.

Table. 4: External field source data imposed on the combo without shielding

External field data			
Q10 (negative or *Vertical*)	-31.5 T/m	220 A (nominal)	300 A
Q11 (positive or *Horizontal*)	24.02 T/m	168 A (nominal)	300 A
Distance Combo-Q10 (center to center)	100 mm		
Distance Combo-Q11 (center to center)	100mm		

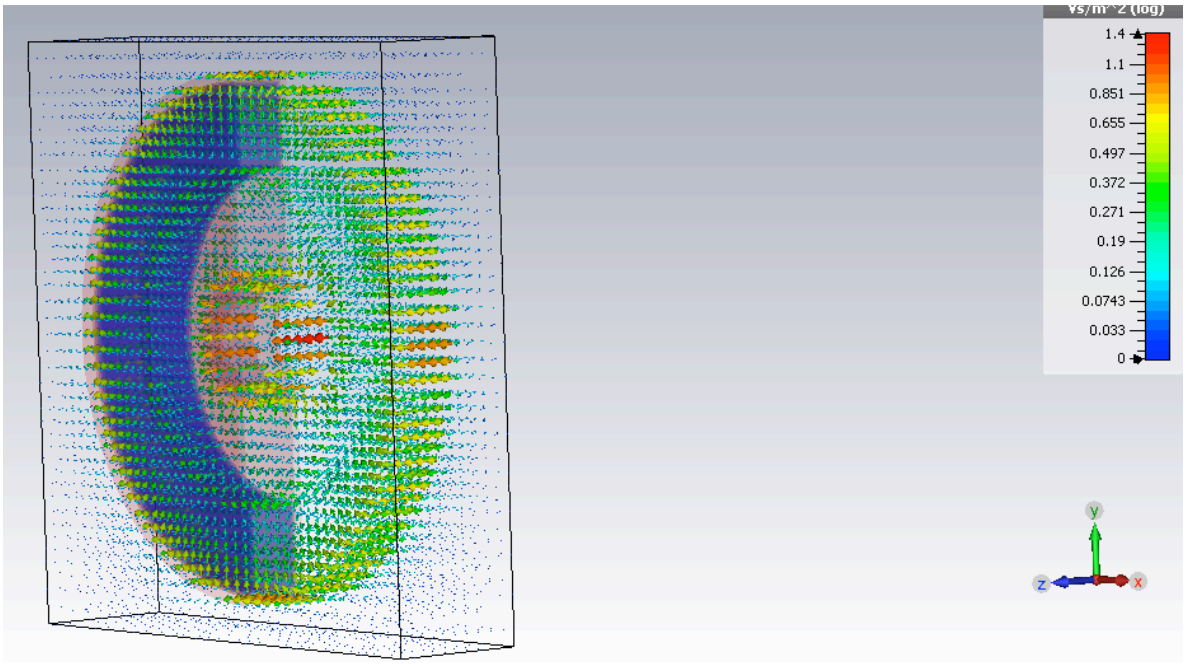

Figure. 5: A 3D model of magnetic field of combo.

4.2.1. INTEGRATED EXTERNAL MAGNETIC FIELDS

Fig.6 shows the external longitudinal magnetic field in the center of combo toroids (i.e ACCT2, FCT). In the Figs [6,7] the three-operation modes of the adjacent quadrupoles have been considered, however the scenario of both positive current of the quadrupoles never will occur during the normal operation of the MEBT.

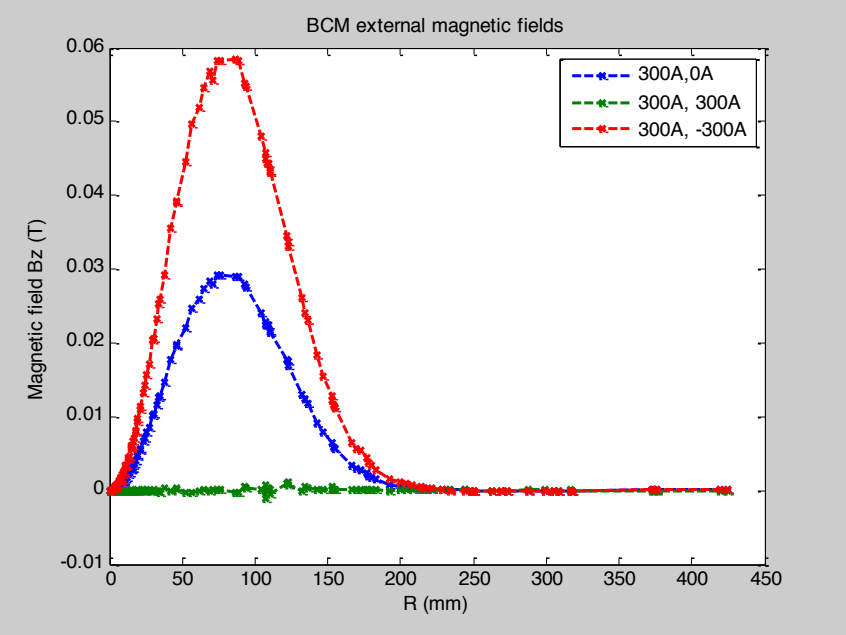

Figure. 6: External longitudinal magnetic field in the center of toroids vs. Radius.

In the Fig.6, the green, blue and red corresponds to [Q10(+) Q11(+),], [Q10(+) Q11(0)], [Q10(+)Q11(-)]. Based on the MEBT lattice '*mebt_2015.v0'*, the nominal operation current of the quadrupoles Q10, Q11 is around [-220A, 168A]. See Fig. 1 and Fig. 2 for the location of quadrupoles Q10 and Q11 in the MEBT. In the Fig. 6, R corresponds to the radiaus from center of the toroid which is located at 100mm from the Q10 center. The graph shows the longitudinal field on the vertical axis (angle of $\pi/2$) in transverse plane.

Fig. 7 shows the external transverse radial magnetic field in the longitudinal-center of toroids.

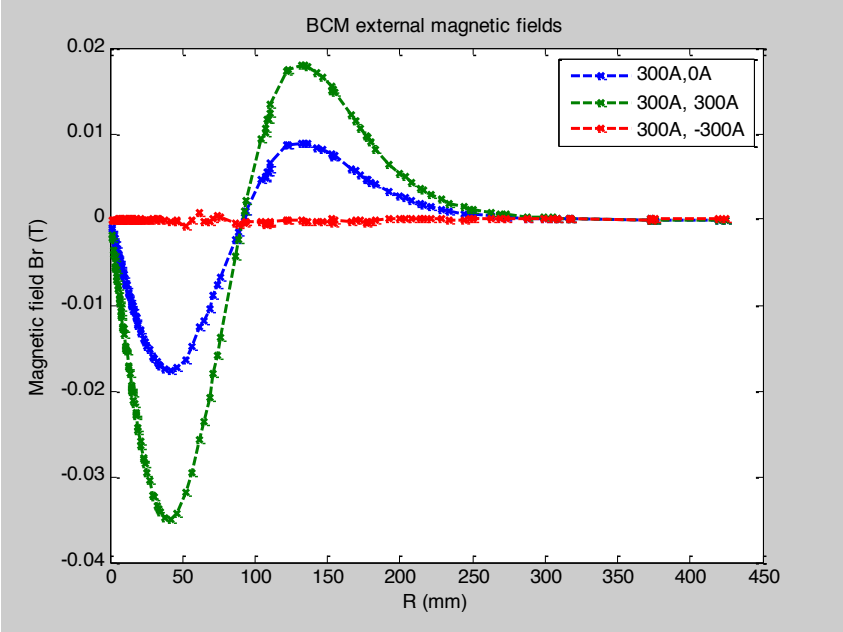

Figure. 7: External transverse radial magnetic field in the center of toroids.

In the Fig. 7, the green, blue and red corresponds to [Q10(+) Q11(+)],[Q10(+) Q11(0)],[Q10(+) Q11(-)]. Based on the MEBT lattice '*mebt_2015.v0',* the nominal operation current of the quadrupoles Q10, Q11 is around[-220A, 168A]. R corresponds to the radiaus from center of the toroid which is located at 100mm from the Q10. The graph shows the radial field on the vertical axis (angle of $\pi/2$) in transverse plane.

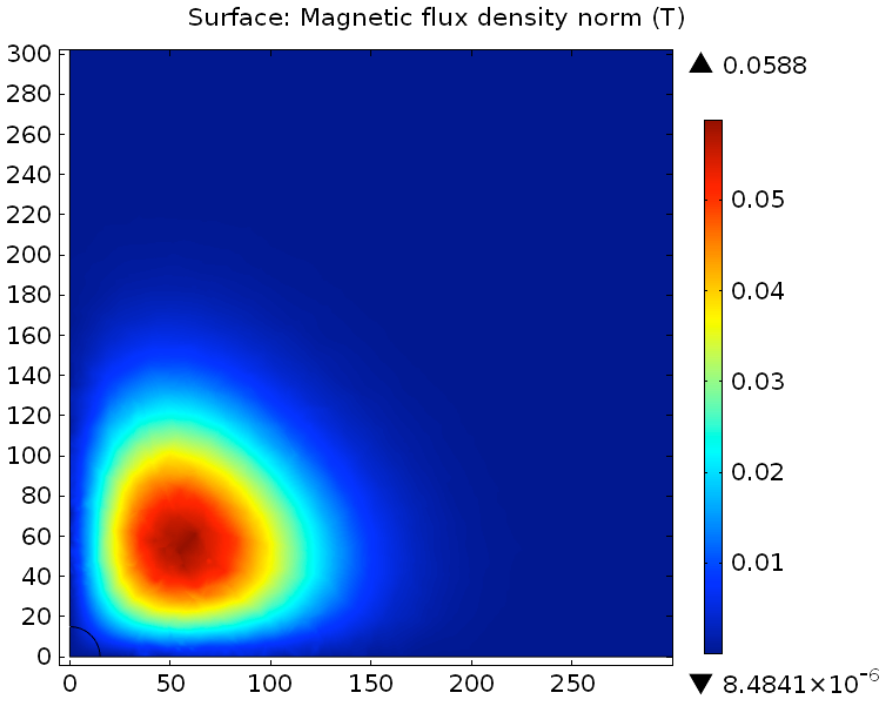

Figure. 8: Absolute magnetic field colour map in the center of toroids. Horizontal/vertical axis correspond to x,y of toroids surface plane.

4.2.2. IN-AIR OPTION

Magnetic field analysis has been performed in order to evaluate the magnetic stray fields from adjacent quadrupoles (i.e Q10, Q11) in the location of the combo. The magnetic data from quadrupoles fields shows the presence of relatively high value of integrated magnetic field (Br, φ) in the location of combo. Figs. [6,7] show the total external magnetic field in the location of combo.

Since the values of magnetic fields are higher than the saturation level of toroids, magnetic shield study has been performed. This magnetic shield will attenuate the external magnetic fields to a value far below 2mT. The overall shield will guarantee the correct readings of beam current by the toroids in particular when proton beam pulse has considerable flat top.

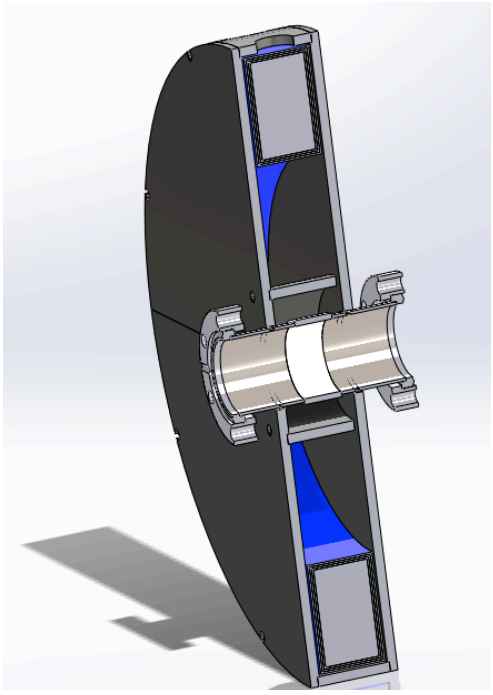

Figure. 9: In-Air option general scheme.

The shielding is based on 1mm Mu-metal foils and 5mm soft iron housing envelope. The thick soft iron will attenuate the external magnetic field with large values, while the Mu-metals are making fine attenuations in low magnetic field region. Due to low saturation level of the Mu-metals, they are not suitable to be used directly as the primary shield of the combo.

Figs. [10,11] show the magnetic permeability graphs of the soft iron and Mu-metal in DC mode.

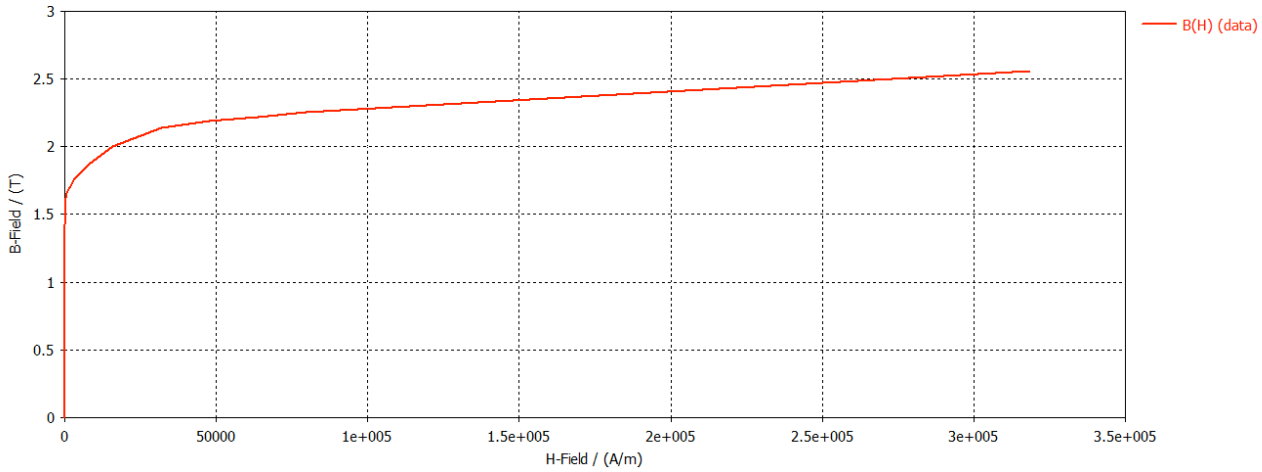

Figure. 10 : Magnetic permeability curve of soft iron.

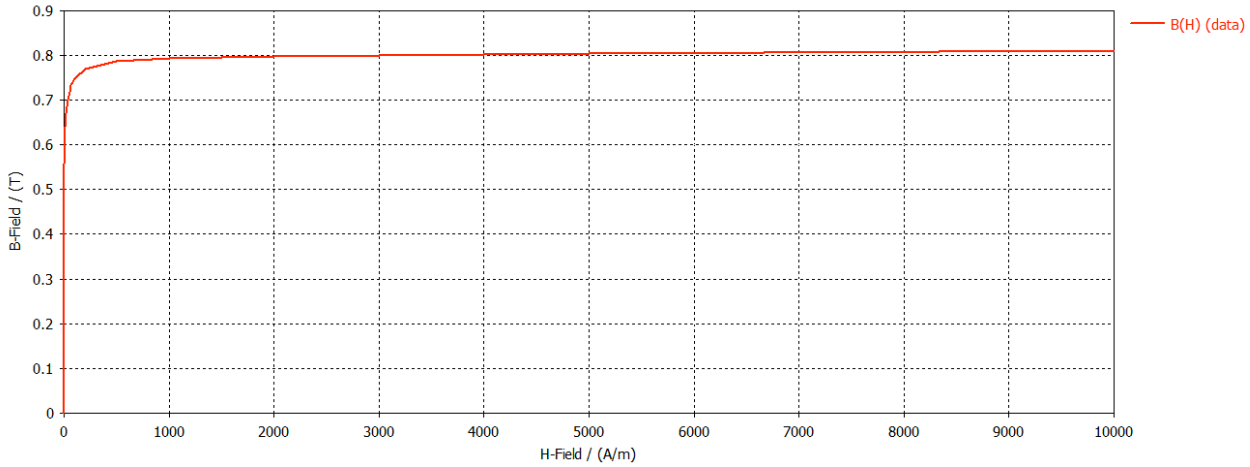

Figure. 11: Magnetic permeability curve of Mu-metal.

Fig. 12 shows the magnetic field attenuation of the external field due to shielding of soft iron in combination with Mu-metals. The attenuation for shielding thickness of 2mm, 4mm and 5mm shows reduction of magnetic field to less than 2-3mT. Reduction of magnetic field from 3 mT to few Gauss is done by the Mu-metal foils (i.e-12 mm <x <12 mm in the Fig. 12)

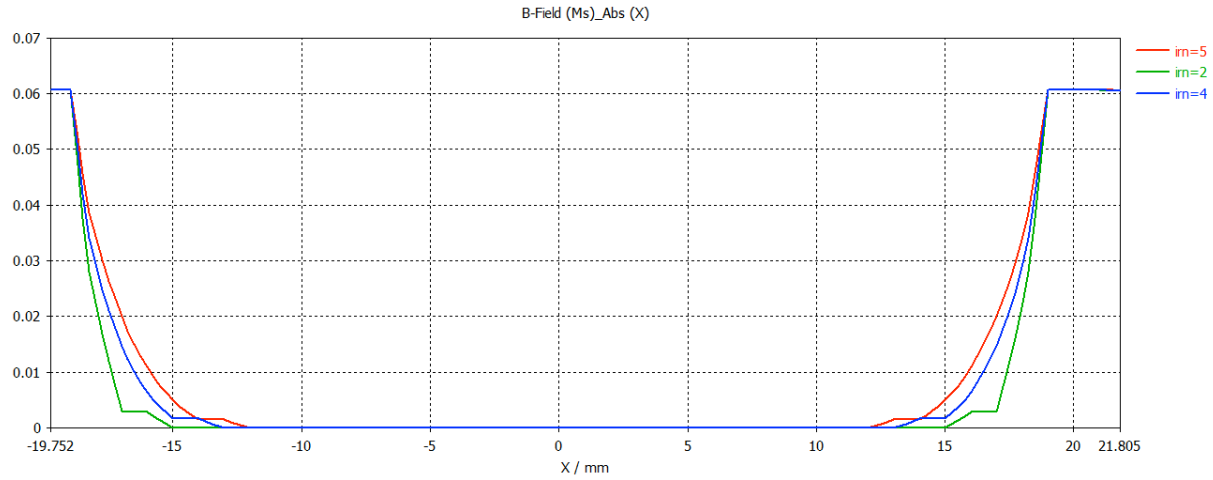

Figure. 12: The external magnetic field attenuation for various shielding thickness of soft iron in combination with Mu-metal.

4.2.3. IN-FLANGE OPTION

In order to reduce the possibility of high frequency noises generated by passage of beam in the shielding cavity and on the other hand having a compact design, an in-vacuum solution is investigated. In this solution, the combo with its Mu-metal foils are integrated in a vacuum flange-flange container. The central part is a customized Bergoz in-flange current transformer with two toroids, with modifications on Mu-metal shielding foils. For the integration purposes of MEBT, the entrance upstream and downstream flanges are rotatable CF40. The outer soft iron shield encloses the whole combo structure with extra screws on the body of combo. Since the bypass path already is in place, the outer shield does not need specific conductivity path. The insulation gap is made of brazed ceramic Al2O3.The internal diameter of FCT and ACCT toroids are 68 mm and 162 mm respectively. Outer diameter of the combo including the outer shield is 260 mm. The ceramic part is brazed to the rest of body, while the other junction parts are welded with TIG. The main advantage of the in-flange option is high frequency noise reduction together with higher bandwidth for FCT. The In-flange combo option has been chosen for the implementation in MEBT.

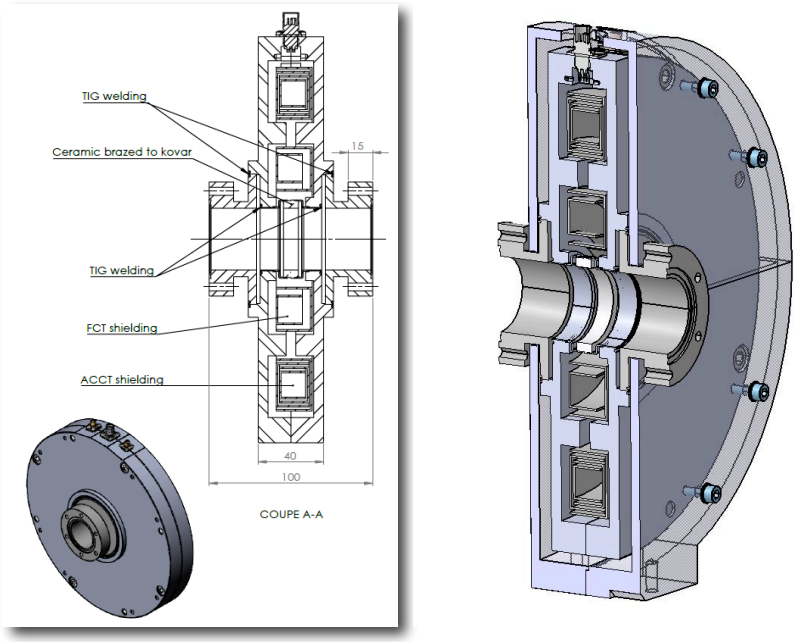

Figure. 13: MEBT BCM combined toroids (left) and enclosed in outer shielding (right).

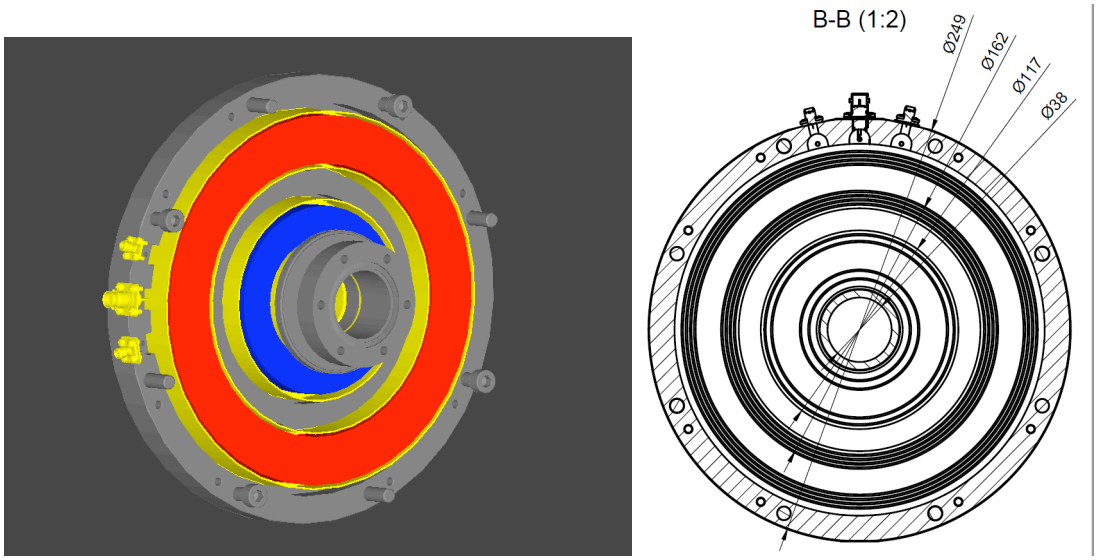

Figure. 14: A 3D view of MEBT Combo, FCT toroid (Blue) and ACCT2 toroid (Red) and toroids diameters (right).

5. SIGNAL CONNECTORS

5.1. FCT SIGNAL CONNECTOR

FCT has one signal connector of SMA type. The connector has female gender and it is located on the outer body of the combo. The connector is accessible from outside for the signal cable connection and disconnection (see Fig. 13).

5.2. ACCT1, ACCT2 CONNECTORS

ACCT1 and ACCT2 have two signal connectors each, as described below.

5.2.1. CURRENT SIGNAL CONNECTOR

The type of connector is BNO. The connector in both cases of in-air and in-flange (ACCT1, ACCT2) is accessible from outside for the sensor to electronics cable connections. In the ACCT1, the sensor connector is rotated by 90 degree, in order to ease the access to the connector from the side-walk in the tunnel.

In the ACCT2, the sensor connector is located on the stainless steel body of the combo and it is accessible from outside for the sensor cable connection and disconnection.

5.2.2. CALIBRATION CONNECTOR

The type of connector is isolated SMA. The connector has female gender. In both cases of in-air and in-flange (ACCT1,ACCT2), it is accessible from outside for the sensor to electronics cable connections. In the ACCT1, the calibration wire connector is rotated by 90 degree, in order to ease the access to the connector from the side-walk in the tunnel.

In the ACCT2, the calibration wire connector is located on the stainless steel body of the combo and it is accessible from outside for the calibrator cable connection and disconnection.

6. SIGNAL CABLES

The cable *Mulrad 2* is used for the connection between the ACCT1, ACCT2 to the electronics.

This halogen-free cable has superior characteristics in terms of radiation and fire resistance. It complies with the ESS standards on safety.

7. DELIVERABLE BY ESS BILBAO

Table. 5 summarizes the items which will be delivered to ESS Lund by ESS Bilbao, based on the description and specifications mentioned in this document.

Table. 5: The deliverable items to Lund

Item	Description	Comments	References in document
ACCT1	In-Air, ID82	Installed within Beam Dump	Section 5.1 Section 3
ACCT2/FCT	Combo In-Flange	Includes the mu-metal layers, soft iron layer and two toroids ACCT and FCT with CF flanges	Section 5.2 Section 3
ACCT1-E cable	20m, Mulrad-2	BNO connectors	Section 6.2.1
ACCT2-E cable	20m, Mulrad-2	BNO connectors	Section 6.2.1
ACCT1 Analogue electronics	Full scale: ±80mA Output: ±10 V	In: BNO female Out: BNC female	Section 3
ACCT2 Analogue electronics	Full scale: ±80mA Output: ±10 V	In: BNO female Out: BNC female	Section 3

8. VERIFICATION AND MEASUREMENTS

In order to deliver the components to ESS Lund, as ready as possible in order to be installed (if required) and be used by upper level subsystems, some verifications will be planned in the factory and some verification will be realized at ESS Bilbao premises.

8.1. FACTORY VERIFICATIONS

The following tests and verification will be done at the factory and the results will be documented and delivered to ESS Lund.

8.1.1. FACTORY VERIFICATION FOR ACCT1

- Frequency response from 5 Hz to 3 MHz.
- Time response to a step to measure the ACCT output rise time.
- Time response to a long pulse, typ. 30 us.
- Differentiation measurement to measure the droop of the ACCT

- Noise measurement

8.1.2. FACTORY VERIFICATION FOR ACCT2

- Frequency response from 5 Hz to 3 MHz.
- Time response to a step to measure the ACCT output rise time.
- Time response to a long pulse, typical 30 us.
- Differentiation measurement to measure the droop of the ACCT
- Noise measurement

8.1.3. FACTORY VERIFICATION FOR FCT

- Frequency response over the full bandwidth
- Time response to a short pulse, typical 250 ps rise time.
- Time response to a step
- Differentiation measurement to measure the droop of the FCT

A certificate of calibration and a vacuum acceptance tests (for combo ACCT2/FCT) including residual gas analysis and leak detection shall be provided with the test results.

8.2. ESS BILBAO VERIFICATIONS

The metrology verifications including the outer dimensions and flange-to-flange errors based on the mechanical drawings will be done at ESS Bilbao. Vacuum leak test will be done by the supplier and verified at ESS Bilbao. The supplier shall guarantee that all fabricated parts shall be helium leak tested and show no detectable leak $>1x10^{-9}$ mbar l s^{-1} . For a reference the contractor can consult Leaking Test description on Section 3.2 of the "ESS Vacuum Handbook Part 4 – Vacuum Test Manual" [5].

9. PROVISIONAL DELIVERY CALENDAR

Table. 6 shows the provisional start and finish dates of the tasks related to the BCM item.

Table. 6: Provisional calendar of the tasks

Item	Start	Finish
Finish design (including Mechanical)	15- July- 2016	15- April- 2017
Detailed drawings (Joint Bilbao with Bergoz)	02- May- 2017	15- June- 2017
Review of the Technical Report	1- June-2017	15-June-2017
Technical Tender Document	14- July- 2017	24- August- 2017
Tender offer/Order	17- Oct- 2017	
FAT	21-Feb- 2017	
Delivery to ESS Bilbao	12-March- 2017	
Verification at ESS Bilbao	2-April- 2018	19- April- 2018
Documentation	2-May- 2018	30- May- 2018
Delivery to Lund ready	10-June- 2018	

10. REFERENCES

[1] D. Cañoto, J. Muñoz, I. Bustinduy “Quadrupole Magnetic Design”

[2] www.bergoz.com

[3] S. Varnasseri, D. De Cos, I. Bustinduy, “Magnetic shielding report for the ACCT1 of ESS MEBT”, MEBT-BI-BC01.01

[4] T. Mora, I . Bustinduy, F. Sordo, “MEBT-BI-MC55-01 (ESS-0087737)”

[5] G. Hulla, “ESS Vacuum Handbook Part 4 – Vacuum Test Manual,” Handbook ESS-0012897, Apr. 2016.